Contribution from the Chemistry Division,
Argonne National Laboratory, Argonne, Illinois 60439

Structural Studies of Precursor and Partially Oxidized Conducting Complexes. 8. A Neutron Diffraction Investigation of Rubidium Tetracyanoplatinate (2:1) Sesquihydrate, $Rb_2[Pt(CN)_4]\cdot 1.5H_2O$[1a]

TIMOTHY R. KOCH,[1b] PAUL L. JOHNSON, and JACK M. WILLIAMS*

Received November 3, 1976 AIC60792F

The crystal and molecular structure of rubidium tetracyanoplatinate (2:1) sesquihydrate, $Rb_2[Pt(CN)_4]\cdot 1.5H_2O$ (RbTCP), has been determined by a single-crystal neutron-diffraction study. The compound RbTCP crystallizes with eight formula units in the space group C_{2h}^6-$C2/c$ with monoclinic cell dimensions a = 12.693 (8) Å, b = 12.809 (8) Å, c = 13.642 (9) Å, and β = 112.22 (4)°. The centrosymmetric space group $C2/c$ was verified by a very satisfactory least-squares refinement. A total of 4108 reflections were averaged to yield 2875 independent reflections (2417 with $F_o^2 > 1\sigma F_o^2$). The structure solved by direct methods and refinement, using full-matrix least-squares techniques, has produced a final $R(F_o^2)$ value of 0.068 using all data. The structure consists of a bent Pt metal atom chain [bond angle 170.97 (4)°] in which the asymmetric unit contains two crystallographically distinct $Pt(CN)_4^{2-}$ groups, two Rb^+ ions, and two H_2O molecules (one O and one H atom are in disorder). Since the intrachain Pt–Pt separation is somewhat long at 3.421 (2) Å, the largely staggered configuration of adjacent $Pt(CN)_4^{2-}$ groups (torsion angles between adjacent tetracyanoplatinate groups range from 29.47 to 35.24°) may be due to $Rb^+\cdots{}^{\delta-}N{\equiv}C$ attractive interactions and hydrogen bonding effects as well as to further reduction of repulsive cyanide π–π interactions. An inversion center occurs at Pt(1), and a twofold rotation axis is present along the b axis of the cell (on which Pt(2) lies). While Pt(1) resides on the c axis, Pt(2) is displaced 0.270 (1) Å normal to c. This bent Pt–Pt chain appears to result from an asymmetric electrostatic environment about Pt(2) involving $Rb^+\cdots{}^{\delta-}N{\equiv}C$ interactions. The role of Rb^+ ion coordination and hydrogen bonding in this structure is discussed. The importance of RbTCP as a precursor in the formation of partially oxidized tetracyanoplatinate (POTCP) complexes is presented in a discussion of POTCP complexes of rubidium.

Introduction

The chemical and physical properties of the potassium tetracyanoplatinates (Pt^{2+}, $Pt^{2.25+}$, $Pt^{2.3+}$, and Pt^{4+}) have been well described in the literature,[2] and we have recently reported the molecular structures of $K_2[Pt(CN)_4]\cdot 3H_2O$,[3] KTCP, cation deficient $K_{1.75}[Pt(CN)_4]\cdot 1.5H_2O$,[4] K(def)TCP, anion deficient $K_2[Pt(CN)_4]Br_{0.3}\cdot 3H_2O$,[5] KCP(Br), and $K_2[Pt(CN)_4Br_2]$,[6] KTCP(Br_2). With the exception of KTCP(Br_2), which contains octahedrally coordinated Pt^{4+} metal atoms, these platinum complexes form unusual Pt–Pt "chains". The partially oxidized salts, K(def)TCP and KCP(Br), have attracted great interest due to their short Pt–Pt separations and their anisotropic metallic conductivity.

In an effort to understand the effect of cation size and charge on the structure of platinocyanide complexes and on the Pt–Pt bond lengths, we have undertaken the preparation and single-crystal diffraction investigation of new tetracyanoplatinate salts. The observed inability to prepare partially oxidized tetracyanoplatinate salts of divalent cations has previously been described,[7] and we have recently completed single-crystal neutron-difraction studies of several nonpotassium tetracyanoplatinate complexes, viz., $Na_2[Pt(CN)_4]Br_2\cdot 2H_2O$,[8] $Ba[Pt(CN)_4]\cdot 4H_2O$,[9] $Cs_2[Pt(CN)_4]\cdot H_2O$,[10] and the first anion deficient organic complex $[C(NH_2)_3]_2[Pt(CN)_4]Br_{0.25}\cdot H_2O$.[11]

The compoud RbTCP is the first precursor Pt^{2+} salt in which we have observed a bent Pt–Pt chain, although we have observed a helical chain in $Cs_2[Pt(CN)_4]\cdot H_2O$.[10] In this paper we discuss the detailed molecular structure of RbTCP and the origin of the Pt chain distortion. We have found that this Pt^{2+} complex is a "starting material" for the newly prepared POTCP salts $Rb_{1.7}[Pt(CN)_4]\cdot 2H_2O$, Rb(def)TCP,[12] and $Rb_2[Pt(CN)_4]Cl_{0.3}\cdot xH_2O$, RbCP(Cl).[13]

Experimental Section

Crystal Preparation. The $Rb_2[Pt(CN)_4]\cdot 1.5H_2O$ was prepared by the addition of rubidium sulfate to barium tetracyanoplatinate in aqueous solution.[12] Large, light-green crystals were grown by slow evaporation, at room temperature[14] (~22 °C), of a saturated aqueous solution in a desiccator over $MgClO_4$.

Unit Cell and Space Group. Earlier x-ray studies[14,15] are summarized in Table I from which preliminary monoclinic unit cell dimensions were derived. Systematic absences were observed for $(h + k)$ odd when considering (hkl) data and l odd when considering $(h0l)$ data. This suggested that the correct space group was either $C2/c$ or Cc. For precise lattice constant determination 23 intense reflections were centered automatically on the neutron diffractometer.[16] The unit cell parameters (at 22 ● 2° with λ 1.142 (1) Å[17]) determined by least-squares fit of the angles 2θ, χ, and ϕ were: a = 12.693 (8) Å, b = 12.809 (8) Å, c = 13.642 (9) Å, β = 112.22 (4)°, and V_c = 2053.21 Å^3. These values agree well with previously reported x-ray lattice parameters (see Table I). The crystal density of 3.18(1) g cm^{-3}, determined by flotation, agrees with the calculated value of 3.21 g cm^{-3}.

Data Collection. A well-formed light-green crystal weighing 84.7 mg (approximately 1.1 × 1.5 × 2.4 mm) was sealed in a lead-glass capillary to avoid possible water loss during data collection. All data were collected with the crystal mounted in a general orientation using an Electronics-and-Alloys four-circle diffractometer at the CP-5 reactor at Argonne National Laboratory. The fully automated diffractometer operates under remote Sigma V computer control.[18]

Using the least-squares determined orientation matrix, data were automatically collected using the θ–2θ step-scan technique with 0.1° step intervals and preset scan ranges of 36–48 steps. Background counts were taken on each side of the peak with both crystal and counter in a stationary position. A total of 4108 reflections were collected to 2θ = 110° and averaging[19] yielded 2875 independent reflections [2417 with $(F_o^2) > 1\sigma(F_o^2)$]. The agreement factor between averaged reflections was $R(F^2)$ = 0.062.[20] Two reference reflections were remeasured after every 50 reflections in order to monitor instrument and crystal stability; their integrated intensities did not vary more than 4% during data collection. Each reflection was corrected for absorption (μ_c = 0.842 cm^{-1}) and the transmission factors ranged from 0.694 to 0.826. Using the absorption corrected integrated intensities the F_o^2 were obtained by application of the following equation:[21]

$$F_o^2 = (\omega I \sin 2\theta)/(I_0 \lambda^3 N^2 V)$$

where I_0 is the incident intensity, λ is the wavelength, ω is the angular velocity of rotation of the crystal, N is the number of unit cells per unit volume, V is the specimen volume, and θ is the Bragg angle. All data were placed on an approximate "absolute scale" by calibration with a well-characterized NaCl crystal as described previously.[22] The variances of F_o^2 were calculated from $\sigma^2(F_o^2) = \sigma_c^2(F_o^2) + (0.06F_o^2)^2$, where $\sigma_c^2(F_o^2)$ is determined from the counting statistics and 0.06 is an added factor which represents about twice the standard deviation of the integrated intensities of the reference reflections.

Table I.[a] Published Structural Data on $Rb_2[Pt(CN)_4]\cdot 1.5H_2O$

Crystal system	Space group	a / γ	b / β	c, Å / γ, deg	ρ_o / ρ_c	Pt–Pt separation, Å	Ref
Monoclinic[b]	C_{2h}^6-$C2/c$	11.91 (7) / 90	12.84 (7) / 99.8	13.62 (7) / 90	3.20 (2)	3.4	Dupont[14]
Monoclinic[b]	C_{2h}^6-$C2/c$	12.670 (4) / 90	12.776 (4) / 112.2	13.572 (4) / 90			Dupont[15]
Monoclinic[c]	C_{2h}^6-$C2/c$	12.693 (8) / 90	12.809 (8) / 112.22 (4)	13.642 (9) / 90	3.18 (1) / 3.21	3.421 (2)	This work

[a] The estimated standard deviations are given in parentheses and refer to the least-significant figures. [b] Single crystal Weissenberg film x-ray data. [c] Single crystal neutron data.

Table II. Final Discrepancy Indices[a]

Data selection	No. of reflections	$R(F_o)$	$R(F_o^2)$	$R_w(F_o^2)$	σ_1
All reflections	2875	0.073	0.068	0.101	1.01
$F_o^2 > 1.0\sigma(F_o^2)$	2417	0.055	0.065	0.097	1.06

[a] See text for explanation of $R(F_o)$, $R(F_o^2)$, $R_w(F_o^2)$, and σ_1.

Structure Solution and Refinement.[19] Initially the structural solution was attempted using the centrosymmetric space group $C2/c$. The structure was solved by using MULTAN[19] from which the positions of the $Pt(CN)_4^{2-}$ groups were obtained. A full-matrix least-squares refinement of the Pt, C, and N positional parameters (with isotropic thermal parameters) was performed. Fourier and difference Fourier maps were then calculated and the remaining Rb, O, and H atoms were located. It appeared at this point that a model in which one H and one O atom were disordered was required. An additional four cycles of least-squares refinement (isotropic thermal parameters) yielded the following discrepancy indices:

$$R(F_o) = \frac{\Sigma||F_o| - |F_c||}{\Sigma|F_o|} = 0.17$$

$$R(F_o^2) = \frac{\Sigma|F_o^2 - F_c^2|}{\Sigma F_o^2} = 0.24$$

and

$$R_w(F_o^2) = \left[\frac{\Sigma w_i|F_o^2 - F_c^2|^2}{\Sigma w_i F_o^4}\right]^{1/2} = 0.29$$

using all data. Then, an additional four cycles of least-squares refinement, including anisotropic thermal parameters and an isotropic extinction parameter,[23] yielded $R(F_o) = 0.090$, $R(F_o^2) = 0.088$, and $R_w(F_o^2) = 0.13$ using all data. Fourier and difference Fourier maps were again calculated and the largest positive peak on the latter Fourier map was only 2% of the largest peak on the Fourier map. These results appeared to support our initial choice of space group $C2/c$ and therefore no attempt was made to refine the data in the space group Cc. The final refinement with anisotropic thermal parameters and anisotropic type 2 extinction[23b] converged yielding the agreement factors given in Table II.

The standard deviation of an observation of unit weight,

$$\sigma_1 = \left[\frac{w_i|F_o^2 - F_c^2|^2}{(n-p)}\right]^{1/2}$$

where n is the number of observations and p the number of parameters varied (viz. 160) in the least-squares refinement, was 1.01 for all the data and the ratio of observations to parameters was ca. 18:1.

The final positional and thermal parameters are given in Table III and the important bond distances and angles in $Rb_2[Pt(CN)_4]\cdot 1.5H_2O$ are given in Table IV. For the least-squares refinement the coherent neutron scattering amplitudes used for Pt, N, C, O, Rb, and H were respectively 0.950, 0.940, 0.665, 0.580, 0.710, and −0.374 all in units of 10^{-12} cm.[24]

In one early least-squares refinement, the rubidium coherent neutron scattering amplitude was initially set at an earlier reported value of 0.85[25] and was then varied in the refinement. The Rb neutron scattering amplitude after four cycles of least-squares refinement decreased to 0.80. This result supports the more recently reported Rb neutron scattering amplitude of 0.710.[24]

Structure Description

The Bent Pt Atom Chain. The crystal structure consists of $Pt(CN)_4^{2-}$ groups which are stacked along the c axis forming a bent Pt atom chain. There are two independent Pt atoms: Pt(1) is located at the origin with site symmetry $\bar{1}$; Pt(2) lies

Table III. Positional and Thermal Parameters for $Rb_2[Pt(CN)_4]\cdot 1.5H_2O$ and Root-Mean-Square Displacements (in Å) of Atoms Along Their Principal Ellipsoidal Axes[a,b]

	10^4x	10^4y	10^4z	$10^4\beta_{11}$	$10^4\beta_{22}$	$10^4\beta_{33}$	$10^4\beta_{12}$	$10^4\beta_{13}$	$10^4\beta_{23}$	$10^3\mu_1$	$10^3\mu_2$	$10^3\mu_3$
Pt(1)	0	0	0	28 (1)	26 (1)	29 (1)	−2 (1)	11 (1)	−2 (1)	138 (2)	148 (2)	157 (2)
Pt(2)	0	211 (1)	2500	42 (1)	25 (1)	30 (1)	0	12 (1)	0	145 (2)	157 (2)	175 (2)
C(11)	1403 (1)	787 (1)	159 (1)	34 (1)	32 (1)	42 (1)	−4 (1)	15 (1)	−4 (1)	146 (2)	164 (2)	188 (2)
C(12)	955 (1)	1279 (1)	5388 (1)	38 (1)	29 (1)	40 (1)	−2 (1)	15 (1)	−1 (1)	154 (2)	165 (2)	182 (2)
C(21)	1677 (1)	229 (1)	2887 (1)	45 (1)	36 (1)	44 (1)	−3 (1)	14 (1)	3 (1)	165 (2)	179 (2)	198 (2)
C(22)	0	1347 (1)	7500	43 (1)	26 (1)	44 (1)	0	17 (1)	0	147 (2)	171 (2)	188 (2)
C(23)	0	1762 (1)	2500	57 (1)	27 (1)	43 (1)	0	17 (1)	0	150 (2)	187 (2)	201 (2)
N(11)	2245 (1)	1207 (1)	259 (1)	44 (1)	46 (1)	73 (1)	−14 (1)	27 (1)	−11 (1)	151 (1)	201 (1)	249 (1)
N(12)	1546 (1)	2006 (1)	5632 (1)	56 (1)	38 (1)	57 (1)	−12 (1)	19 (1)	−4 (1)	158 (1)	214 (1)	218 (1)
N(21)	2653 (1)	257 (1)	3108 (1)	48 (1)	66 (1)	71 (1)	−7 (1)	18 (1)	3 (1)	179 (1)	231 (1)	252 (2)
N(22)	0	2254 (1)	7500	61 (1)	29 (1)	70 (1)	0	26 (1)	0	154 (2)	204 (2)	238 (2)
N(23)	0	2671 (1)	2500	82 (1)	28 (1)	65 (1)	0	22 (1)	0	151 (2)	227 (2)	249 (2)
Rb(1)	2344 (1)	2697 (1)	2014 (1)	57 (1)	57 (1)	52 (1)	−9 (1)	17 (1)	−12 (1)	179 (2)	209 (2)	234 (2)
Rb(2)	3783 (1)	869 (1)	5560 (1)	56 (1)	46 (1)	57 (1)	−6 (1)	20 (1)	−4 (1)	183 (2)	207 (2)	217 (2)
O(1)	4384 (1)	1532 (2)	103 (2)	52 (1)	56 (1)	76 (1)	−8 (1)	30 (1)	−9 (1)	178 (2)	210 (2)	254 (2)
O(2)[c]	4652 (4)	357 (3)	2575 (3)	70 (3)	51 (2)	67 (3)	0 (2)	26 (3)	−2 (2)	206 (4)	222 (4)	235 (5)
H(1)	3707 (3)	1506 (3)	248 (3)	73 (3)	72 (2)	86 (3)	1 (2)	42 (2)	8 (2)	202 (4)	239 (4)	271 (4)
H(2)	4832 (4)	2065 (4)	547 (4)	98 (3)	85 (3)	122 (4)	−30 (3)	24 (3)	−29 (3)	206 (4)	303 (5)	341 (6)
H(3)	5000	1052 (5)	2500	150 (7)	71 (4)	98 (5)	0	18 (5)	0	243 (7)	271 (7)	360 (9)
H(4)[c]	5980 (7)	391 (6)	2208 (6)	79 (6)	66 (4)	80 (5)	1 (4)	30 (4)	−3 (4)	232 (8)	237 (8)	257 (8)

[a] The estimated standard deviations in parentheses for this and all subsequent tables refer to the least significant figure. [b] The form of the temperature factor is $\exp\{-(\beta_{11}h^2 + \beta_{22}k^2 + \beta_{33}l^2 + 2\beta_{12}hk + 2\beta_{13}hl + 2\beta_{23}kl)\}$. [c] Atoms in crystallographic disorder and multipliers were adjusted appropriately for partial occupancy.

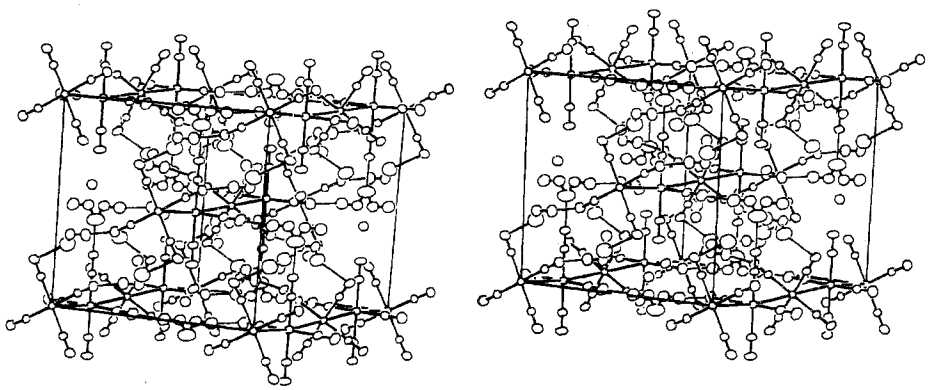

Figure 1. The unit cell drawing of $Rb_2[Pt(CN)_4]\cdot 1.5H_2O$ showing the nonlinear Pt–Pt chain which extends along *c* and has equivalent Pt–Pt separations [3.421 (2) Å and bond angle 170.97 (4)°]. Thermal ellipsoids are scaled to enclose 50% probability. An inversion center occurs at Pt(1) and Pt(2) is displaced 0.270 Å perpendicular to the *c* axis in the +*b* direction. Hydrogen bonds from H_2O to cyanide group nitrogen atoms (H···N < 2.5 Å) are indicated by faint lines.

Table IV. Interatomic Distances (Å) and Bond Angles (deg) for $Rb_2[Pt(CN)_4]\cdot 1.5H_2O$[a]

(A) Distances around Platinum Atoms			
Pt(1)-Pt(2)	3.421 (2)	Pt(2)-C(21)	1.990 (2)
Pt(1)-C(11)	1.985 (2)	Pt(2)-C(22)	1.995 (2)
Pt(1)-C(12)	1.988 (2)	Pt(2)-C(23)	1.987 (2)
(Pt-C) av	1.989 (4)		
(B) Carbon–Nitrogen Distances in Cyanide Groups			
C(11)-N(11)	1.158 (2)	C(21)-N(21)	1.159 (2)
C(12)-N(12)	1.161 (2)	C(22)-N(22)	1.162 (2)
(C-N) av	1.161 (3)	C(23)-N(23)	1.164 (2)
(C) Rubidium Ion Interactions			
Rb(1)-N(12)	3.004 (3)	Rb(2)-H(1)	3.068 (4)
Rb(1)-N(11)	3.027 (2)	Rb(2)-N(12)	3.117 (2)
Rb(1)-H(1)	3.039 (5)	Rb(2)-H(2)	3.118 (6)
Rb(1)-O(1)	3.055 (3)	Rb(2)-N(23)	3.130 (2)
Rb(1)-N(22)	3.180 (3)	Rb(2)-N(21)	3.199 (3)
Rb(1)-N(23)	3.284 (2)	Rb(2)-N(12)	3.226 (2)
Rb(1)-N(21)	3.285 (3)	Rb(2)-N(11)	3.231 (2)
Rb(2)-O(1)	2.923 (3)	Rb(2)-H(4)[b]	3.270 (8)
Rb(2)-O(2)[b]	2.990 (5)	Rb(2)-O(1)	3.285 (3)
Rb(2)-O(2)[b]	3.010 (5)		
(D) Water Molecule O-H Bond Distances			
O(1)-H(1)	0.952 (4)	O(2)[b]-H(3)	1.016 (8)
O(1)-H(2)	0.946 (5)	O(2)[b]-H(4)[b]	0.95 (1)
(E) Hydrogen Bond Distances and Angles			
O(1)-N(11)	2.833 (3)	O(1)-H(1)-N(11)	165.7 (4)
H(1)-N(11)	1.900 (4)		
O(1)-N(12)	3.172 (3)	O(1)-H(2)-N(12)	133.7 (5)
H(2)-N(12)	2.444 (5)		
O(1)-N(22)	3.434 (3)	O(1)-H(2)-N(22)	131.3 (4)
H(2)-N(22)	2.735 (6)		
O(2)[b]-N(21)	2.896 (5)	O(2)[b]-H(4)[b]-N(21)	170.9 (7)
H(4)[b]-N(21)	1.948 (8)		
O(2)[b]-N(22)	3.100 (5)	O(2)[b]H(3)-N(22)	151.2 (3)
H(3)-N(22)	2.170 (7)		
(F) Angles within the Platinocyanide Groups			
Pt(1)-C(11)-N(11)	177.1 (1)	Pt(2)-C(22)-N(22)	180
Pt(1)-C(12)-N(12)	177.7 (1)	Pt(2)-C(23)-N(23)	180
C(11)-Pt(1)-C(12)	87.58 (7)	C(21)-Pt(2)-C(22)	89.31 (5)
Pt(2)-C(21)-N(21)	178.9 (1)	C(21)-Pt(2)-C(23)	90.69 (5)
		C(22)-Pt(2)-C(23)	180
(G) Angles within the Water Molecules			
H(1)-O(1)-H(2)	105.3 (5)	H(3)-O(2)[b]-H(4)[b]	116.0 (6)

[a] All distances are uncorrected for thermal motion. [b] This atom is in crystallographic disorder and only the chemically reasonable interatomic distances are given (see text).

Table V. Nitrogen Atom Interactions (Interatomic Distances in Å)

(A) Nitrogen Atoms in the Pt(1) $(CN)_4^{2-}$ Group			
N(11)-H(1)	1.900 (4)	N(12)-H(2)	2.444 (5)
N(11)-O(1)	2.933 (3)	N(12)-Rb(1)	3.004 (3)
N(11)-Rb(1)	3.027 (2)	N(12)-Rb(2)	3.117 (2)
N(11)-Rb(2)	3.231 (2)	N(12)-O(1)	3.172 (3)
		N(12)-Rb(2)	3.226 (2)
(B) Nitrogen Atoms in the Pt(2) $(CN)_4^{2-}$ Group			
N(21)-H(4)[a]	1.948 (8)	N(22)-O(2)[a]	3.100 (5)
N(21)-O(2)[a]	2.896 (5)	N(22)-O(2)[a]	3.100 (5)
N(21)-Rb(2)	3.199 (3)	N(22)-Rb(1)	3.180 (3)
N(21)-Rb(1)	3.285 (3)	N(22)-Rb(1)	3.180 (3)
N(21)-Rb(1)	3.420 (3)	N(23)-Rb(2)	3.130 (2)
N(22)-H(3)	2.170 (7)	N(23)-Rb(2)	3.130 (2)
N(22)-H(2)	2.735 (6)	N(23)-Rb(1)	3.284 (2)
N(22)-H(2)	2.735 (6)	N(23)-Rb(1)	3.284 (2)

[a] This atom is in crystallographic disorder and only the chemically reasonable interatomic distances are given (see text).

on a twofold rotation axis and is displaced perpendicular to the *c* axis (along the *b* axis) by 0.270 (1) Å. The bent Pt atom chain thus comprises Pt(1) and Pt(2) [bond angle 170.97 (4)°] as illustrated in the stereodiagram of the unit cell in Figure 1. All Pt–Pt bond lengths are equal at 3.421 (2) Å as required by symmetry.

The $Pt(2)(CN)_4^{2-}$ group appears to be displaced from the *c* axis by asymmetric Rb^+ ion interactions as shown in the stereodiagram in Figure 2. We have observed such a result previously for the smaller K^+ cations in the POTCP complex $K_{1.75}[Pt(CN)_4]\cdot 1.5H_2O$.[4] Electrostatic interactions of N(23) with four surrounding Rb^+ ions clearly appear to override the combination of the electrostatic attraction between N(22) and two Rb^+ ions and three hydrogen bonds to N(22) (the environments surrounding these N atoms are listed in Table VB). Consequently, the $Pt(2)(CN)_4^{2-}$ group is displaced along the *b* axis in the direction of N(23).

The $Pt(CN)_4^{2-}$ Groups. The asymmetric unit of the crystal contains two crystallographically independent $Pt(CN)_4^{2-}$ groups, two Rb^+ ions, and two H_2O molecules (one O and one H atom are in disorder). The $Pt(1)(CN)_4^{2-}$ and $Pt(2)(CN)_4^{2-}$ groups are nearly planar as shown in Table VI in which the best least-squares planes for these groups are presented.

The $Pt(1)(CN)_4^{2-}$ group is not truly square [the angle C(11)–Pt(1)–C(12) is 87.58 (7)°]. Again this appears to be due to an asymmetric Rb^+ ion distribution surrounding N(11) and N(12), most significantly in the *ab* plane normal to Pt(1) (the environments surrounding these N atoms are listed in Table VA). In comparison, because of the nearly symmetric Rb^+ ion distribution within the *ab* plane normal to Pt(2), similar distortion of the $Pt(2)(CN)_4^{2-}$ group is not nearly as great [the angle formed by C(21)–Pt(2)–C(22) is 89.31 (15)°].

The Pt–C bond distances within the tetracyanoplatinate groups are all within 2σ of the average Pt–C bond length

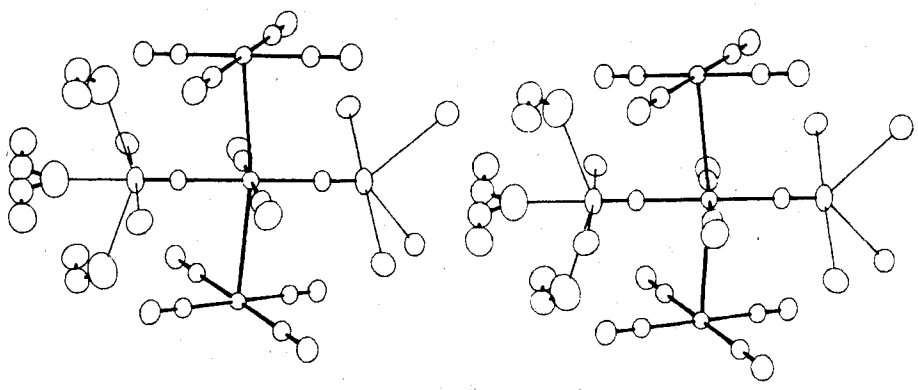

Figure 2. The asymmetric crystalline environment about Pt(2). All Rb^+ ions neighboring Pt(2) cyanide nitrogen atoms to 3.3 Å are included. In addition a 3.3 Å coordination sphere about Pt(2) cyanide nitrogen atoms, which lie in special positions along a twofold rotation axis, is included. The crystallographic c axis is vertical and $+b$ is to the right. The four Rb^+ ions which interact with N(23) are shown in the $+b$ direction.

Table VI. Least-Squares Planes for the $Pt(CN)_4^{2-}$ Groups, Perpendicular Distances (Å) from These Planes, and Dihedral Angles in RbTCP[a,b]

(A) Plane I through Pt(1), C(11), C(12), N(11), and N(12)

$0.2099X - 0.1637Y - 0.9639Z = 0$

Pt(1)	0 (0)	N(11)	0.002 (1)
C(11)	−0.002 (1)	N(12)	0.006 (1)
C(12)	−0.009 (1)		

(B) Plane II through Pt(2), C(21), C(22), C(23), N(21), N(22), and N(23)

$0.2444X - 0.9697Z = 3.3767$

Pt(2)	0 (0)	N(21)	0.002 (1)
C(21)	−0.002 (1)	N(22)	0 (0)
C(22)	0 (0)	N(23)	0 (0)
C(23)	0 (0)		

(C) Dihedral Angles, deg

$Pt(1)(CN)_4^{2-}$ plane with ab plane of the unit cell:	13.7
$Pt(2)(CN)_4^{2-}$ plane with ab plane of the unit cell:	8.1

[a] In each of the equations of the plane, X, Y, and Z are coordinates (Å) corresponding to the orthogonal axes a, b, and c^*. [b] The sense of the distances given is that + corresponds to the +c.

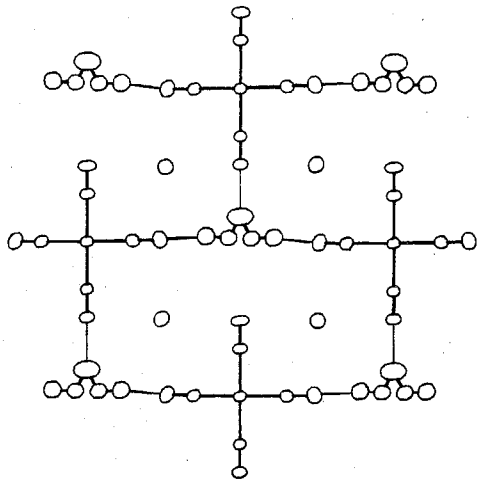

Figure 3. View of the ab section perpendicular to Pt(2) showing the hydrogen bonding of the $H_2O(2)$ sites which are in crystallographic disorder (see text). Water molecule to cyanide nitrogen atom hydrogen bonds (H···N < 2.5 Å) are indicated by faint lines. The Rb^+ ions are shown without bonding interactions.

[1.989 (4) Å] (see Table IVA). As an indication of the precision of this study the C≡N bond distances are identical to within 1σ of the average value [1.161 (3) Å] (see Table IVB).

The torsion angles between the tetracyanoplatinate groups (angles formed by C–Pt(1)–Pt(2)–C) range from 29.5 to 35.2°. These large torsion angles could indicate considerable cyanide group repulsion between adjacent $Pt(CN)_4^{2-}$ groups in the stack. However, the long Pt–Pt separation (3.421 (2) Å) suggests that other factors may be involved. In contrast, the torsion angles of $K_2[Pt(CN)_4]\cdot 3H_2O$, which has a Pt–Pt separation of 3.478 (1) Å, range from 15.7 to 16.7°.[3] One might expect that in Pt atom stacks which have long Pt–Pt bond lengths, the $Pt(CN)_4^{2-}$ groups could assume almost any torsion angle. The observed configuration in such tetracyanoplatinate complexes seems to result from $M^+\cdots^{\delta-}N{\equiv}C$ attractions (where M^+ is the cation present) and hydrogen bonding rather than strictly from π–π cyanide group repulsion. The influence of $M^+\cdots^{\delta-}N{\equiv}C$ and hydrogen bonding interactions might be best determined by comparing several different hydrates of a tetracyanoplatinate complex. An x-ray diffraction study[26] of $Rb_2[Pd(CN)_4]\cdot H_2O$ (isomorphic with $Rb_2[Pt(CN)_4]\cdot H_2O$) has shown that upon the loss of $0.5H_2O$, the Pd–Pd bond length has increased by ~0.3 Å to 3.72 (1) Å. Using the x-ray atomic positional parameters,[26] calculations[19] show that the torsion angles between adjacent $Pd(CN)_4^{2-}$ groups range from 15.7 to 16.8°. By comparison of the structure of $Rb_2[Pt(CN)_4]\cdot 1.5H_2O$ with that of $Rb_2[Pd(CN)_4]\cdot H_2O$, it is seen that in the latter the Pd–Pd bond length has increased by ~0.3 Å to 3.72 (1) Å and that the torsion angles have concomitantly decreased to 15.7–16.8°. A complete structural study of $Rb_2[Pt(CN)_4]\cdot H_2O$ is needed to better understand these relationships.

H_2O Disorder and Hydrogen Bonding in $Rb_2[Pt(CN)_4]\cdot 1.5H_2O$. It was discovered that the oxygen positions suggested by Dupont in a previous single-crystal x-ray diffraction study[15] were incorrect. The positional parameters listed for the O(1) site are incorrect by ~5 Å along the c axis. In addition, the O(2) site was not shown to be disordered as we have discovered.

The disordered oxygen atoms [O(2)′ and O(2)″] and the disordered hydrogen atoms [H(4)′ and H(4)″] are respectively related by a symmetry element. The remaining hydrogen atom, H(3), is situated on a twofold rotation axis. The H_2O molecule appears to pivot about the H(3)–N(22) vector (the N···H distance is 2.170 (7) Å) and cross-links $Pt(2)(CN)_4^{2-}$ groups on adjacent Pt atom chains as shown in Figure 3. Similar cross-linking, again due to H_2O disorder, was observed in $K_{1.75}[Pt(CN)_4]\cdot 1.5H_2O$.[4]

The nondisordered water molecule, $H_2O(1)$, basically cross-links $Pt(1)(CN)_4^{2-}$ groups on adjacent Pt atom chains as shown in Figure 4. The H(1)···N(11) bond is the shortest hydrogen bond in the structure [1.900 (4) Å]. The second hydrogen atom, H(2), participates in bifurcated hydrogen bond formation by bonding to N(12) [N···H = 2.444 (5) Å] and

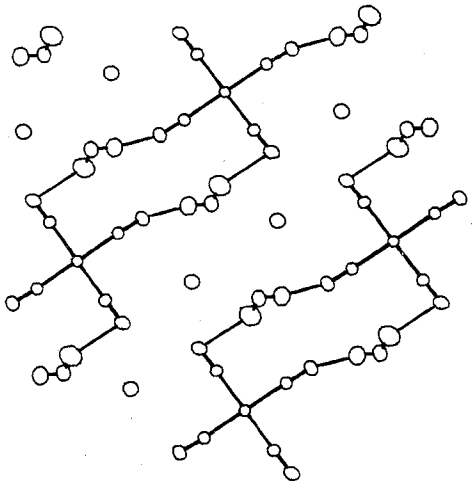

Figure 4. View of the *ab* section perpendicular to Pt(1) showing hydrogen bonding of the $H_2O(1)$ molecule linking $Pt(1)(CN)_4^{2-}$ groups. Water molecule to cyanide nitrogen atom hydrogen bonds (H···N) < 2.5 Å) are indicated by faint lines. The Rb^+ ions are given without bonding interactions.

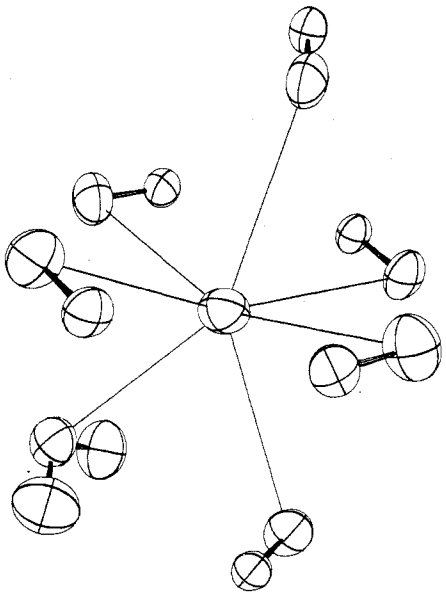

Figure 5. The $Rb^+(1)$ coordination sphere in $Rb_2[Pt(CN)_4]\cdot 1.5H_2O$. Interactions with an oxygen atom (Rb···O < 3.2 Å) and cyanide nitrogen atoms (Rb···N < 3.5 Å) are indicated by faint lines.

by additionally forming a weaker hydrogen bond with N(22) [2.735 (6) Å] in the adjacent $Pt(2)(CN)_4^{2-}$ group.

Structural Comparisons of POTCP Precursor Compounds. $Rb_2[Pt(CN)_4]\cdot 1.5H_2O$, $K_2[Pt(CN)_4]\cdot 3H_2O$, and $Cs_2[Pt(CN)_4]\cdot H_2O$. In $K_2[Pt(CN)_4]\cdot 3H_2O$ (KTCP) the $Pt(CN)_4^{2-}$ groups are stacked perpendicularly to the *c* axis forming linear Pt–Pt atom chains as required by symmetry considerations [Pt–Pt = 3.478 (1) Å, orthorhombic space group *Pbcn*].[3] The coordination about the K^+ ion in KTCP is sevenfold with four N and three O nearest neighbors. We have found that with the larger Rb^+ ion present, interactions of the type $Rb^+\cdots {}^{\delta-}N{\equiv}C$ can cause distortion of the Pt atom chain. As shown in Figure 5, the coordination about Rb(1) is also sevenfold but with six N and one O near neighbors. The coordination about Rb(2) is eightfold with five N and three O near neighbors (the $H_2O(2)$ site is in disorder) as shown in Figure 6. Distortion of the Pt–Pt atom chain due to cationic interactions with the cyanide nitrogen atoms has also been observed in $Cs_2[Pt(CN)_4]\cdot H_2O$ in which we have found a novel helical

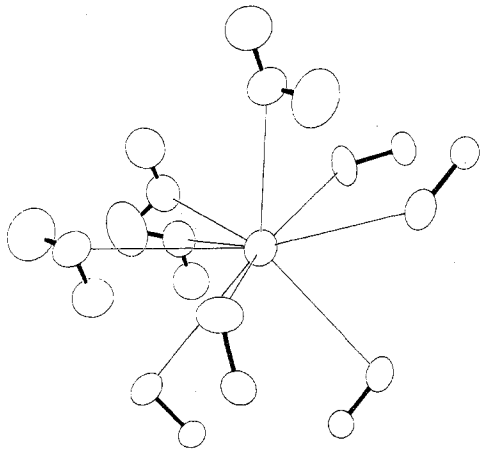

Figure 6. The $Rb^+(2)$ ion coordination sphere in $Rb_2[Pt(CN)_4]\cdot 1.5H_2O$. Interactions with oxygen atoms [the $H_2O(2)$ site is in disorder] (Rb···O < 3.4 Å) and cyanide nitrogen atoms (Rb···N < 3.5 Å) are indicated by faint lines.

Pt–Pt atom chain.[10] There are two Cs^+ ion sites and the coordination of Cs(1) ion is eightfold with seven N and one O nearest neighbor. The coordination of the second Cs^+ ion site is sevenfold with six N and one O nearest neighbor.

Discussion and Conclusions

The compound $Rb_2[Pt(CN)_4]\cdot 1.5H_2O$ (RbTCP) is a starting material in the preparation of a partially oxidized complex having the approximate composition $Rb_{1.7}[Pt(CN)_4]\cdot 2H_2O$, Rb(def)TCP.[12] An anion deficient rubidium complex, $Rb_2[Pt(CN)_4]X_{0.3}\cdot yH_2O$ (X = Cl, Br), has previously been reported several times.[13,27,28] However, we have found that the cocrystallization (at ~22 °C) of RbTCP with $Rb_2[Pt(CN)_4X_2]$ ($X = Br^-$) yields bronze needles identified by powder x-ray diffraction[29] and chemical analyses[30,31] as Rb(def)TCP. These results support the reaction shown in eq 1. This proposed reaction (see eq 1) is further supported by

$$\sim 7Rb_2[Pt(CN)_4]\cdot 1.5H_2O + Rb_2[Pt(CN)_4X_2] \xrightarrow{H_2O} \sim 8Rb_{1.7}[Pt(CN)_4]\cdot 2H_2O + 2RbX\ (X = Br^-) \quad (1)$$

the observation that cocrystallization of RbBr and Rb(def)TCP yields a mixture of light-green and yellow crystals thought to be RbTCP and $Rb_2[Pt(CN)_4Br_2]$. In contrast, cocrystallization of $K_{1.75}[Pt(CN)_4]\cdot 1.5H_2O$ and KBr yields bronze needles that have been identified by powder x-ray diffraction analysis[32] as the well-known complex $K_2[Pt(CN)_4]Br_{0.3}\cdot 3H_2O$.[33] It has also been suggested[34] that a low-temperature cocrystallization (<10 °C) of RbTCP with $Rb_2[Pt(CN)_4Br_2]$ yields the partially oxidized complex $Rb_2[Pt(CN)_4]Br_{0.23}\cdot xH_2O$. However, when this cocrystallization was carried out at ~4 °C, bronze needles were formed which were shown to contain no bromine by chemical analysis.[31] Therefore, it appears that in the case of anion deficient POTCP salts of rubidium only Cl^- and not Br^- complexes have been prepared to date.

In the literature, there are no substantiated reports of partially oxidized tetracyanoplatinate complexes grown from nonaqueous solution. The hydrogen bonding which interlinks $Pt(CN)_4^{2-}$ chains in RbTCP (see Figures 3 and 4) suggests that a solvent that forms suitably strong hydrogen bonds could possibly be used in the crystallization of POTCP complexes. We are therefore presently attempting to crystallize partially oxidized rubidium tetracyanoplatinate complexes in solvents such as methanol and formamide. It is hoped that these new solvents will further separate adjacent Pt atom chains and thus influence interchain interactions. Organic cations may also

prove to be useful in interlinking Pt atom chains. A single-crystal neutron-diffraction study of the anion deficient guanidinium complex, $(C(NH_2)_3)_2[Pt(CN)_4]Br_{0.25}\cdot H_2O$,[11] has recently shown that an organic cation can stabilize tetracyanoplatinate complexes by hydrogen bonding interactions.

A complete molecular study of $Rb_2[Pt(CN)_4]\cdot 1.5H_2O$ has shown many structural features which we have previously found in the partially oxidized Pt salt, $K_{1.75}[Pt(CN)_4]\cdot 1.5H_2O$. Square-planar tetracyanoplatinate complexes in each case stack to form chains of Pt atoms. Distortion of the Pt atom chain in each structure is due to an asymmetric distribution of cations in the crystal lattice. In addition, cross-linking of adjacent Pt atom chains by a disordered water molecule has been observed in both structures.

Acknowledgment. We wish to thank Elizabeth Gebert for assistance with powder x-ray diffraction experiments, D. M. Washecheck for assistance with the ORTEP figures, and J. P. Faris for spectrographic analyses performed at Argonne.

Registry No. $Rb_2[Pt(CN)_4]\cdot 1.5H_2O$, 16985-46-9.

Supplementary Material Available: Listing of structure factor amplitudes (10 pages). Ordering information is given on any current masthead page.

References and Notes

(1) (a) This work was performed under the auspices of the U.S. Energy Research and Development Administration. (b) Student sponsored in part by the Argonne Center for Educational Affairs from Coe College, Cedar Rapids, Iowa, and by the Argonne Chemistry Division.
(2) See, for example, J. S. Miller and A. J. Epstein, *Prog. Inorg. Chem.*, **20**, 1 (1976).
(3) D. M. Washecheck, S. W. Peterson, A. H. Reis Jr., and J. M. Williams, *Inorg. Chem.*, **15**, 74 (1976).
(4) J. M. Williams, K. D. Keefer, D. M. Washecheck, and N. P. Enright, *Inorg. Chem.*, **15**, 2446 (1976).
(5) J. M. Williams, J. L. Petersen, H. M. Gerdes, and S. W. Peterson, *Phys. Rev. Lett.*, **33**, 1079 (1974); J. M. Williams, F. K. Ross, M. Iwata, J. L. Petersen, S. W. Peterson, S. C. Lin, and K. D. Keefer, *Solid State Commun.*, **17**, 45 (1975); J. M. Williams, M. Iwata, F. K. Ross, J. L. Petersen, and S. W. Peterson, *Mater. Res. Bull.*, **10**, 411 (1975).
(6) D. M. Washecheck, P. L. Johnson, T. R. Koch, and J. M. Williams, submitted for publication.
(7) T. R. Koch, E. Gebert, and J. M. Williams, *J. Am. Chem. Soc.*, **98**, 4017 (1976).
(8) R. L. Maffly, P. L. Johnson, T. R. Koch, and J. M. Williams, *Acta Crystallogr.*, in press.
(9) R. L. Maffly, P. L. Johnson, and J. M. Williams, *Acta Crystallogr.*, submitted.
(10) P. L. Johnson, T. R. Koch, and J. M. Williams, *Acta Crystallogr.*, submitted.
(11) J. M. Williams, T. F. Cornish, D. M. Washecheck, and P. L. Johnson, *Amer. Crystallogr. Assoc. Abstr.*, **4**, 59 (1976).
(12) For the preparation of this platinum salt see, T. R. Koch, J. A. Abys, and J. M. Williams, *Inorg. Synth.*, **19**, in press.
(13) We have prepared this salt by aqueous electrolysis (with Pt electrodes) of $Rb_2[Pt(CN)_4]\cdot 1.5H_2O$ in the presence of RbCl.
(14) L. Dupont, *Bull. Soc. Roy. Sci., Liege*, **36**, 40 (1967). It is reported herein that the compound $Rb_2[Pt(CN)_4]\cdot H_2O$, orthorhombic and colorless, crystallizes when the ambient temperature is greater than 26 °C.
(15) L. Dupont, *Bull. Soc. R. Sci., Liege*, **38**, 509 (1969).
(16) A. J. Zielen, P. Day, and J. M. Williams, Proceedings and Abstracts of the Neutron Diffraction Meeting, Petten, The Netherlands, 1975, pp, 38 and 39.
(17) The monochromatic neutron beam is produced by reflection from the (110) plane of a Be single crystal at a monochromator angle of θ_m = 30°. Calibration of the neutron wavelength of 1.142 (1) Å was made with two standard cubic crystals: NaCl (a = 5.6397 Å) and Si (a = 5.430 Å) at 22 ± 2 °C. Measurements of the neutron flux at the sample position with calibrated Au foils yielded an intensity of 2.9×10^6 N cm^{-2} s^{-1}.
(18) P. Day and J. Hines, *Operating Systems Rev.*, **7**, 28 (1973).
(19) The computer programs which were used in performing the necessary calculations, with their accession names in the World List of Crystallographic Computer Programs (3d ed), are as follows: data reduction and absorption corrections, DATALIB; data averaging and sort, DATASORT; Fourier summation, FORDAP; least-squares refinement, OR XLFS3; error analysis of distances and angles, OR FFE3, and structural drawings, OR TEPII. For determination of least-squares planes the program PLNJO was used; J.-O. Lundgren, University of Uppsala, Uppsala, Sweden; based on the method of D. Blow, *Acta. Crystallogr.*, **13**, 168 (1960). For the direct methods solution MULTAN was used; J. P. Declercq, G. Germain, P. Main, and M. M. Woolfson, *Acta. Crystallogr., Sect. A*, **29**, 231 (1973).
(20) The agreement factor after averaging equivalent data and based on F_o^2 is defined as $R(F_o^2) = \sum(F_{av}^2 - F_o^2)/\sum F_o^2$.
(21) S. W. Peterson and H. A. Levy, *Acta Crystallogr.*, **10**, 70 (1957).
(22) J. L. Petersen, L. F. Dahl, and J. M. Williams, *J. Am. Chem. Soc.*, **96**, 6610 (1974).
(23) The Zachariasen approximation[23a] was used for the overall isotropic g parameter as defined and scaled by Coppens and Hamilton.[23b] The $|F_o|$ values were corrected for extinction from the expression $|F_o|_{corr} = |F_o|(1 + \bar{T}2g\lambda^3|F_c|^2/V^2 \sin 2\theta)^{-1/4}$, where $|F_c|$ is on an absolute scale, λ is the wavelength (Å), g is the refined extinction parameter, $\bar{T}$ is mean absorption-weighted path length in the crystal in centimeters (calculated simultaneously during the computation of absorption corrections), and V is the unit cell volume (Å^3). (a) W. H. Zachariasen, *Acta Crystallogr.*, **23**, 558 (1967); (b) P. Coppens and W. C. Hamilton, *Acta Crystallogr., Sect. A*, **26**, 71 (1970).
(24) G. E. Bacon, *Acta Crystallogr., Sect. A*, **28**, 357 (1972).
(25) G. E. Bacon, *Acta Crystallogr., Sect. A*, **25**, 391 (1969).
(26) L. Dupont, *Acta Crystallogr., Sect B*, **26**, 964 (1970).
(27) For reports of $Rb_2[Pt(CN)_4]Cl_{0.3}\cdot xH_2O$, see: (a) K. Krogmann, N.A.T.O. Advanced Study Institute on Chemistry and Physics of One-Dimensional Metals, Aug. 17–29, 1976, Bolzano, Italy; and (b) A. E. Underhill, D. M. Watkins, and D. J. Wood, to be published.
(28) For reports of $Rb_2[Pt(CN)_4]Br_{0.25}\cdot xH_2O$, see: (a) R. Comès, M. Lambert, H. Launois, and H. R. Zeller, *Phys. Rev. B.*, **8**, 571 (1973); (b) H. R. Zeller, *Festkoerperprobleme*, **13**, 31 (1973); and (c) D. Kuse, *Solid State Commun.*, **13**, 887 (1973).
(29) Comparison was made with the x-ray powder pattern of an authentic sample of Rb(def)TCP which was prepared as described in ref 12.
(30) All chemical analyses were performed by Midwest Microlab, Indianapolis, Ind.
(31) Chemical analyses for halogen always indicated that trace amounts (<0.1%) or no halogen was present.
(32) Comparison was made with the x-ray diffraction powder pattern of an authentic sample of $K_2[Pt(CN)_4]Br_{0.3}\cdot 3H_2O$.
(33) For a definitive study of this compound, see ref 5.
(34) Private communication with H. R. Zeller, Brown, Boveri & Co., Ltd., Baden, Switzerland.